Catalysis Today 260 (2016) 3–7

Contents lists available at ScienceDirect

Catalysis Today

journal homepage: www.elsevier.com/locate/cattod

Surface segregation and oxidation of $Pt_3Ni(1\,1\,1)$ alloys under oxygen environment

H.C. Lee[a,1], B.M. Kim[b,1], C.K. Jeong[b], R. Toyoshima[c], H. Kondoh[c], T. Shimada[d], K. Mase[e], B. Mao[f], Z. Liu[f], H. Lee[g], Chuan-Qi Huang[h], W.X. Li[h,*], P.N. Ross[f], B.S. Mun[a,i,**]

[a] Department of Physics and Photon Science, School of Physics and Science, Gwangju Institute of Science and Technology , Republic of Korea
[b] Department of Applied Physics, Hanyang University, ERICA, Republic of Korea
[c] Department of Chemistry, Keio University, Tokyo, Japan
[d] Department of Science, Faculty of Education, Hirosaki University, Aomori, Japan
[e] Institute of Materials Structure Science, High Energy Accelerator Research Organization, 1-1 Oho, Tsukuba, Ibaraki 305-0801, Japan
[f] Advanced Light Source, Lawrence Berkeley National Laboratory, Berkeley, CA 94720, USA
[g] Department of Chemistry, Sookmyung Women's University, Seoul, Republic of Korea
[h] State Key Laboratory of Catalysis, Dalian Institute of Chemical Physics, Chinese Academy of Sciences, Dalian 116023, China
[i] Ertl Center for Electrochemistry and Catalysis, Gwangju Institute of Science and Technology, Republic of Korea

ARTICLE INFO

Article history:
Received 25 February 2015
Received in revised form 3 May 2015
Accepted 5 May 2015
Available online 6 June 2015

Keywords:
Ambient pressure XPS
Pt alloys
Metal oxidation
DFT
Surface segregation

ABSTRACT

Utilizing ambient pressure X-ray photoelectron spectroscopy (AP-XPS), the surface segregation and oxidation of $Pt_3Ni(1\,1\,1)$ alloys are investigated as a function of temperature and oxygen pressure. The *in situ* AP-XPS measurements of oxygen oxidation process show that the Pt "skin" surface is not stable under the exposure of oxygen pressure of 100 mTorr at room temperature. As the temperature and pressure are elevated, the formations of Ni_2O_3, NiO_x, and NiO are observed on surface while Pt atom starts to reduce its adsorbed oxygen, which is a clear sign of surface segregation of Ni to surface. Upon the evacuation of oxygen gas, *i.e.* ultrahigh vacuum condition, both of NiO_x and NiO oxide get reduced and Ni_2O_3 remains on the surface. The DFT calculation is employed to explain the formation of surface oxides under oxidation condition.

Among many candidates for next generation fuel cells, the polymer membrane fuel cell (PMFC) shows many advantages over other competing ones, including low temperature operation and environmental friendliness. However, a slow oxygen reduction rate (ORR) at cathode in PMFC remains as the main obstacle, and the high cost of Pt as a cathode material limits the practical applications of hydrogen fuel cell technology. Although no substitutes for Pt have yet been found for catalytic materials for cathode materials in fuel cell, the recent reports [1,2] have shown that the rate of ORR in PMFC is improved by 80 times when the Pt is alloyed with certain 3*d* transition metals (TM) at around 25% of total concentration. The reports showed the presence of Pt "skin" layer (Pt-Skin) formed during electrochemical measurements, and further pointed out the altered surface electronic structures from the formation of the Pt skin layer as the origin of the enhanced chemical reactivity [3,4].

Immediately after the reports came out, tremendous amounts of efforts have been devoted to fabricate or synthesize the material that can reproduce or mimic the chemical reactivity found in model system. In the meantime, it has been shown that reactivity of surface can be controlled by adjusting the degrees of TM metal surface segregation, based on the thermodynamics and kinetics of bimetallic systems under oxygen exposure. Out of immense investigations, many groups in this field learn that the structure of Pt skin layer is not stable under reaction conditions and the subsurface 3*d* TM can be easily segregate to the surface layer under the operating conditions [5,6]. The TM has higher electronegativity than Pt and it segregates to the surface under the elevated oxygen pressure and even at low temperature, leading to the degradation of surface reactivity. As well known, the stability in electrochemistry is one of the critical factors to consider for its successful application to fuel cell. Consequently, the issues of surface segregation of TM in Pt_3TM system and its loss of reactivity have become the most important problems to resolve [7,8].

* Corresponding author at : Dalian Institute of Chemical Physics, Chinese Academy of Sciences, Dalian, China.
** Corresponding author at: Department of Physics and Photon Science, Ertl Center for Electrochemistry and Catalysis, Gwangju Institute of Science and Technology, Republic of Korea.
E-mail addresses: wxli@dicp.ac.cn (W.X. Li), bsmun@gist.ac.kr (B.S. Mun).
[1] These authors contributed equally to this work.

http://dx.doi.org/10.1016/j.cattod.2015.05.003
0920-5861/

Previously, the stability of Pt-3*d* TM system was investigated with DFT calculation, showing the structural evolution under various reaction conditions [7]. According to the report, Pt-skin surface is more stable under reductive condition, *i.e.* ultrahigh vacuum condition (UHV) and CO conditions, while 3*d* TM-skin surface become more stable under oxidizing condition. Furthermore, the group looked into the case of oxygen induced segregation of $Pt_3Ni(1\,1\,1)$ system and calculated the corresponding phase diagram [8]. According to their calculation, under UHV condition, the Pt-skin surface is energetically more stable. However, with increase of oxygen chemical potential, the stronger O—Ni bonding strength can overcome the cost of segregation energy and the surface forms Ni-enriched surface layer with oxygen coverage higher than 0.50 ML. One thing to note here is that Pt skin surface is not stable in the argument of surface energy, *i.e.* Pt has higher surface energy compared to the one of the Ni. In the case of this particular system, strain effect can explain the situation better. Pt atoms in Pt_3Ni bulk are under the compressive strain compared to the Pt bulk parent, whereas Ni atoms in Pt_3Ni are under the expansive strain compared to the Ni bulk parent. Accordingly, compared to their bulk parents, the surface energy for Pt-skin of Pt_3Ni would decrease because of stronger inner-layer interaction under the compressive strain, but for Ni skin of Pt_3Ni increase under the expansive strain. This might lead to the Pt-skin more favorable than that of the Ni-skin, as found in experiment, though opposite to the order of the Pt and Ni surface energies/cohesive energies for their bulk parents.

In the meantime, in 2013, with the use of XPS, X-ray absorption spectroscopy (XAS), and electron energy loss spectroscopy, A. Politano et al. reported the evidence of Ni segregation and the formation of NiO_x surface oxide upon the exposure of $Pt_3Ni(1\,1\,1)$ surface to the oxygen gas at surface temperature of 600 K [9]. The group measured the Ni *3p* core-level XPS spectra and Ni *L*-edge XAS spectra to demonstrate the evidence of surface segregation and oxidation of Ni elements in $Pt_3Ni(1\,1\,1)$. The conclusion of the report is that the oxygen atom bonds on Ni atom, showing no sign of Pt associated to oxygen as expected. However, it is to note that the entire measurements of the report are carried out by means of *ex situ* measurement, *i.e.* the process of oxidization was carried out separately prior to the measurements and entire measurements are carried out under UHV condition. In addition, the group used the analysis of Ni *3p* core-level peak for extracting the oxidation state information. However, in this particular system, Ni *3p* level is not suitable choice for identifying exact oxidation state since the Ni *3p* peak heavily influenced by the background of Pt *4f* peak in the Pt_3Ni alloys.

In early 2014, C. Chen et al. reported the successful fabrication of 3-dimenstional Pt_3Ni nanoframes exhibiting nano-segregated Pt-skin structures with both enhanced reactivity and durability [10]. The group fabricates the open-framework structures composed of 2 ML of Pt-covered surface with Ni atom inside by transforming the $PtNi_3$ polyhedra to Pt_3Ni nanoframes with preferential etching under solution. Interestingly, this group utilized the Ni segregation property under oxygen pressure to produce the Pt-skin layer out of nanoframes and made it stable under reaction condition. This report demonstrated that the surface segregation effects can be well utilized so that ideal surface composition can be achieved in nano-scale alloys system.

In this report, we present the real-time *in situ* measurement of surface segregation of Ni atoms on $Pt_3Ni(1\,1\,1)$ surface under oxygen pressurized condition. With ambient pressure X-ray photoelectron spectroscopy (AP-XPS), the *in situ* measurements of oxygen oxidation process are carried out on $Pt_3Ni(1\,1\,1)$ surface and the stability of Pt "skin" surface is examined as a function of temperature and pressure. In order to resolve the oxidation states of Ni during the segregation/oxidation processes, both of O *1s* and Ni *2p* core-level spectra are measured simultaneously

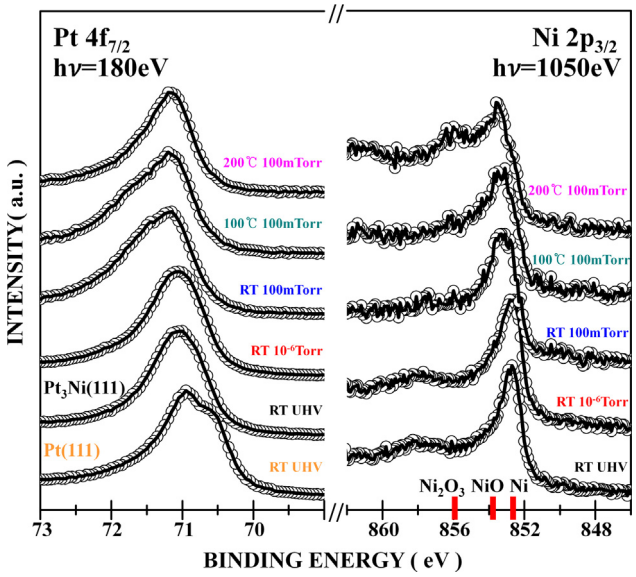

Fig. 1. Pt *4f* and Ni *2p* core-level spectra measured as a function of oxygen gas pressure and temperature.

under *in situ* oxidizing condition. At room temperature, there is no clear indication of Ni segregation to surface up to the oxygen pressure of 10^{-6} Torr. However, as the oxygen pressure is increased to 100 mTorr at room temperature, the Ni_2O_3 and NiO_x oxide starts to appear at the surface. When the sample temperature is increased to 100 °C under 100 mTorr of oxygen pressure, the NiO oxide starts to form on the surface. All the portion of Ni-oxides compounds, Ni_2O_3, NiO_x, and NiO, continuously grow when the surface temperature is further increased to 200 °C. Upon the removal of oxygen gas to UHV, *i.e.* the reducing condition, both of NiO_x and NiO oxide get reduced significantly, yet Ni_2O_3 oxide becomes significantly increased. To understand the thermodynamics of oxidation processes in $Pt_3Ni(1\,1\,1)$, DFT calculation is employed.

The AP-XPS measurements are carried out at soft-ray beamline BL13 at Photon-Factory of High Energy Accelerator Research Organization (KEK-PF) in Tsukuba, Japan [11] and BL9.3.2 at Advanced Light Source of Lawrence Berkeley National Laboratory, USA [12]. The details of AP-XPS endstations on both synchrotron radiation facilities can be found elsewhere [13]. The $Pt_3Ni(1\,1\,1)$ single crystal is provided by MaTek Inc. and the clean surface is prepared with repeated cycles of sputtering and annealing processes as previously described in the literature [4]. The surface cleaning cycle was repeated until no trace of carbon and oxygen species are detected by XPS. Before the experiment, the surface condition was checked by LEED and the well-ordered LEED patterns are observed, identical to previous report [4]. The gas pressure was controlled by UHV metal leak valve and the sample heating was made by using pyrolytic boron nitride (PBN) heater from the backside of sample.

For theoretical calculation, spin-polarized density functional theory calculations were performed using Vienna Ab-initio Simulation Package (VASP) [14,15], employing the all-electron projected augmented wave (PAW) potentials [16,17], and the Perdew-Wang 91 (PW91) exchange-correlation functional [18]. The wave function was expanded by plane wave with kinetic cutoff of 400 eV. A grid of $(12 \times 12 \times 12)$ Monkhorst-Pack grid (containing the Γ point) was used for the Brillouin zone k points sampling for bulk calculation. The optimized lattice constants for the bulk Pt (fcc), NiO (rock salt), and Pt_3Ni ($L1_2$) are 3.99, 4.19, 3.89 Å, respectively. The total energy of O_2 was corrected by using the experimental enthalpy of water [19].

First, Fig. 1 shows the normalized Pt *4f* and Ni *2p* core-level spectra as a function of temperature and the oxygen pressure. The Pt *4f* peak of Pt(1 1 1) surface is also shown as comparison in the bottom. Under UHV condition, Pt *4f* of Pt_3Ni(1 1 1) shows the presence of surface state on lower binding energy side, which corroborates nicely with the formation of the Pt-skin surface. The degree of core-level shift of this surface state is however smaller compared to the one of the Pt(1 1 1) in below and this is due to hybridization of Pt and Ni atoms at the surface layer [4]. Consistent with the observation, the Ni *2p* spectra on the right hand side also shows clear metallic features, *i.e.* binding energy at 852.9 eV and the satellite shoulder at higher binding energy side at 858.0 eV [20]. As the pressure increase to 10^{-6} Torr, the surface state of Pt *4f* clearly gets decreased and the peak shoulder of higher binding energy side starts to increase slightly, indicating that oxygen starts to adsorb on the surface whereas the Ni *2p* spectra are essentially same with the one under UHV. Considering that pure Ni(1 1 1) surface can be immediately oxidized to form at least 3 ML NiO under 100 L of oxygen gas [21], the intact metallic features of Ni atom observed under 10^{-6} Torr here tells that Ni atoms remain below the Pt-skin surface at this condition., *i.e.* no exposure to oxygen.

Under 100 mTorr of oxygen pressure in Fig. 1, the intensity of higher binding energy side of Pt *4f* spectrum shows further enhancement, indicating the increase of chemisorbed oxygen on surface. In the case of Ni *2p* spectra, the position of leading peak edge is shifted to higher binding energy side and the metallic satellite feature at 858.0 eV is diminished. Though it remains unclear whether Ni-oxide is being formed based on the given spectra alone, the diminishing of the metallic feature of Ni tells an oxygen-induced surface segregation occurs already in this pressure regime at room temperature. In fact, it is possible to predict the formation of oxidic oxygen on Ni. Further analysis on the oxidic oxygen from Ni and oxygen induced segregation will be discussed later with the O *1s* spectra which are taken under the identical condition shown in Fig. 2.

Once the pressure reaches to 100 mTorr, the temperature is increased from room temperature to 100 and 200 °C in sequence. At $T = 100$ °C, Pt *4f* and Ni *2p* spectra shows almost identical features as the one from room temperature. However, the peak shoulder of higher binding energy side of Pt *4f* is clearly increased and the peak position of leading edge in Ni *2p* spectra is clearly shifted away from the metallic position of Ni at 852.9 eV. When the temperature is further increased to 200 °C, Pt *4f* starts to show reduction of its intensity near chemisorbed oxygen position, Pt—O_{ads}. This could possibly mean that the chemisorbed oxygen on Pt starts to desorb under higher temperature. Or, it is also possible that Ni segregates to surface interfering the further interaction of Pt to external oxygen gases or even starts interact the adsorbed oxygen on Pt atoms. In the Ni spectra, there are now two distinct Ni *2p* peaks at 853.6 and 856.00 eV appeared, which are the sign for the formation of NiO and Ni_2O_3 oxides [20]. However, the peak assignment out of our Ni *2p* spectra requires a careful attention since the interpretation of Ni *2p* core-level spectra involves non-local core-hole screening and complex electronic structure of Ni oxide system [22].

Therefore, in order to confirm the presence of oxides and resolve its chemical state in more convincing way, O *1s* spectra are measured under 100 mTorr as a function of surface temperature, shown in Fig. 2. With 100 mTorr of oxygen at room temperature, total four oxygen species are found. Two oxygen species at 529.8 eV and 533.00 eV belong to the chemisorbed oxygen attached Pt (Pt—O_{ads}) and CO on surface, respectively. The CO comes from the chamber wall at long exposure of elevated gas pressure. However, the amount of CO is reduced significantly at the elevated pressure of oxygen as the high pressure washes away the weakly bound CO on surface. The estimated coverage of CO is less than 0.1 ML. The other two oxygen species at 530.8 eV and 531.5 eV are identified as

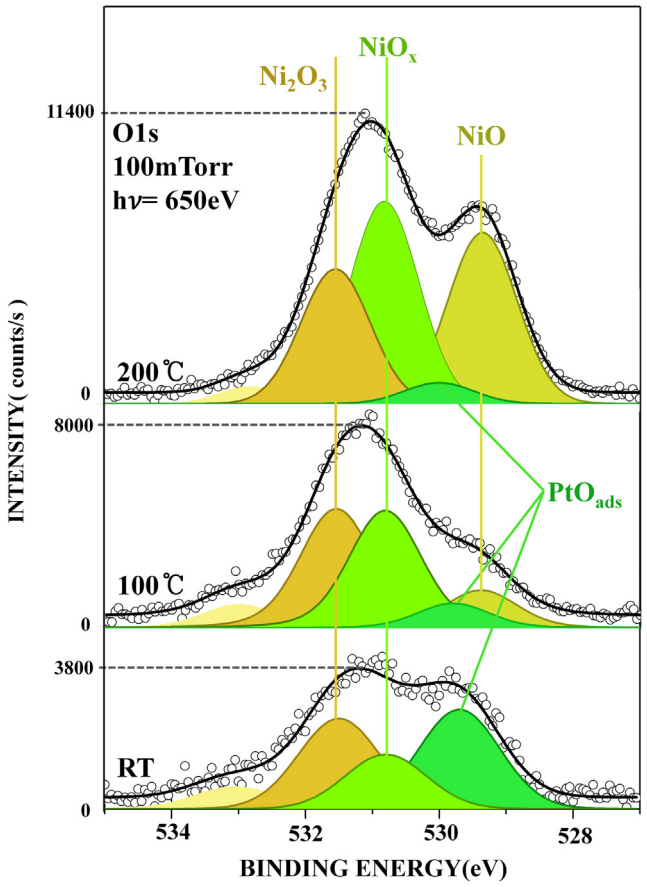

Fig. 2. O *1s* core-level spectra measured as a function of temperature at 100 mTorr of oxygen gas pressure.

NiO_x and Ni_2O_3 surface oxide respectively. Oxygen in NiO_x is the additional oxidic oxygen species mentioned in Ni *2p* of Fig. 1. There is a possibility of forming Pt oxide, *i.e.* PtO_x, under this oxidation condition. Previously, Miller et al. [23] reported the Pt(1 1 1) oxidation study using AP-XPS and showed the surface oxide formed under similar pressure and temperature condition. However, the position of O *1s* from surface oxide in the report does not show identical core-level shift as that of PtO_x in Fig. 2. Previously, it is reported [4] that the adsorption energy of oxygen on Pt_3Ni(1 1 1) surface is weaker than Pt(1 1 1) surface due to the presence of Ni atoms near distance and the formation of Pt surface oxide is very unlikely under this condition.

At 100 °C, both O *1s* signal from NiO_x and Ni_2O_3 surface oxide shows significant enhancement and, more importantly, NiO start to appear at 529.4 eV. Previously, the presence of Ni-oxides is also suspected from Ni *2p* spectra in Fig. 1. Also, Pt—O_{ads} gets decreased as the temperature increase while NiO_x increases continuously. When the temperature was further increased to 200 °C, the formation of NiO is further activated and its amount outgrows amount of Ni_2O_3. In the meantime, NiO_x grows continuously, which can be understood the NiO_x as a precursor species to NiO. Overall, the analysis of Figs. 1 and 2 confirms the presence of the surface segregation and the formation of surface oxides and the Pt-skin layer is no longer stable under oxygen pressure.

In order to understand the growth mechanism, the depth profile information on these oxides is achieved by varying the kinetic energy of detected photoelectrons, *i.e.* varying excitation energy of incoming photon. By varying the kinetic energy of outgoing electron, the surface sensitivity of XPS information can be tuned. Since no LEED pattern was observed after the oxide was grown on surface,

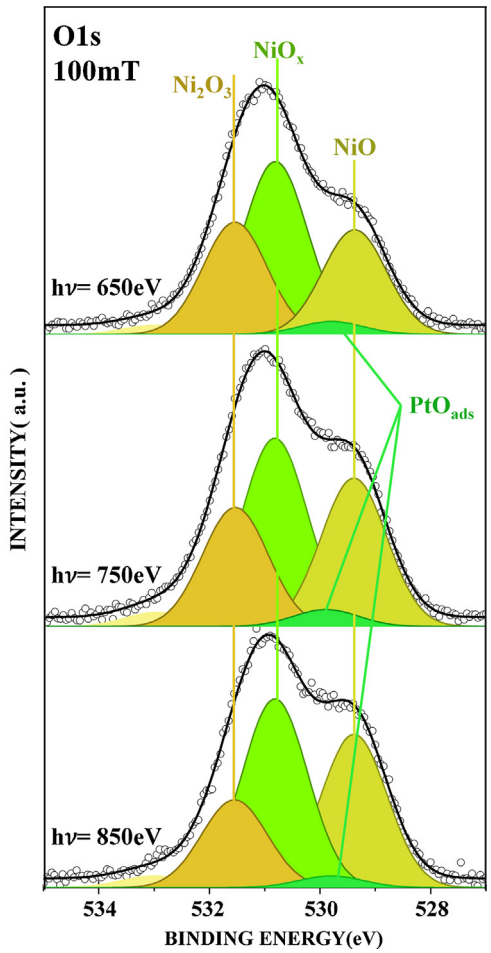

Fig. 3. O *1s* core-level spectra measured at different photon excitation energies at 100 mTorr of oxygen gas pressure and $T = 200\,^{\circ}C$.

it is expected that photoelectron diffraction effect is minimum. In Fig. 3, the three different photon energies are used to excite the O *1s* spectra, 650 eV, 750 eV, and 850 eV, which is corresponds to 6–9 Å of inelastic mean free path of electrons [24]. Fig. 3 shows that intensity of NiO_x and NiO oxides increase as the photon energy is increased while Ni_2O_3 shows the opposite behavior. The Ni_2O_3 intensity is decreased by 20% from 750 eV to 850 eV of photon energy. That is, more of NiO and NiO_x oxides stay further below surface while Ni_2O_3 oxide forms near surface layer. This observation is consistent with the previous report in which that Ni_2O_3 is only stable on the surface region. According to the report of Kim et al., the Ni_2O_3 species formed mainly on the surface at the high temperature oxidation processes, and is considered as the gross surface defect structures of NiO [20]. This information provides an interesting oxidation processes on this alloy system. Namely, Ni_2O_3 and NiO_x is being formed first on the surface and, then NiO is being formed below the surface only after high pressure of oxygen and temperature are reached. Considering the melting temperatures of these two elements [25], *i.e.* 1960 °C for NiO and 600 °C for Ni_2O_3, one could assume that the formation energy of Ni_2O_3 would be lower than NiO. However, the above melting temperatures are only valid for the relative stability of bulk phase, and the caution needs to be paid in the case of surface oxidation. The analysis of Figs. 1 and 2 obviously shows that Ni_2O_3 always formed first, and more resistant to decomposition. We note that for the oxide growth of Rh(1 1 1) under high temperature and pressure [26], RhO_2 surface oxide is being formed as intermediate states and prevents further oxidation at intermediate pressure condition. At elevated pressure condition, stable Rh_2O_3 oxide is being formed, which is exactly opposite to the result of this Pt_3Ni alloy system.

To rationalize the experimental results, we studied the feasibility of oxygen induced phase separation of Pt_3Ni and formation of NiO and Pt in bulk counterpart. The corresponding heat of formation energy ΔH per NiO mole was calculated using DFT at absolute zero according to following formula:

$$Pt_3Ni\,(bulk) + 0.5O_2 \rightarrow 3Pt\,(bulk) + NiO\,(bulk) + \Delta H$$

and the calculated $\Delta H = -1.28$ eV/NiO. The exothermic ΔH indicates that the phase separation of Pt_3Ni (bulk) and formation of NiO in the presence of oxygen is energetically favorable. Taking into account of the entropy effect of oxygen in gas phase at given temperature T and partial pressure P, the corresponding Gibbs free energy of formation ΔG could be approximated by *ab initio* thermodynamics [27–29] *via*

$$\Delta G = \Delta H - 0.5\,\Delta\mu(O_2, T, P) = \Delta H - 0.5\,\Delta\mu(O_2, T, P^0) - 0.5k_BT\,\ln(P/P^0)$$

where $\Delta\mu\,(O_2, T, P^0)$ is the chemical potential of oxygen at given T [25].

For the present experimental condition applied, $T = 100$ and 200 °C ($P = 100$ mTorr), the calculated ΔG are −0.75 and −0.59 eV/NiO, respectively. It can be seen that for these experimental conditions, the corresponding ΔG remain exothermic. Namely, even considering the entropy effect of oxygen, the formation of NiO from Pt_3Ni is still thermodynamically favorable. These results substantiate the observation of NiO signals at $T = 100$ and 200 °C ($P = 100$ mTorr). At RT, the calculated ΔG (−0.89 eV/NiO) becomes even more exothermic than those at higher T (100 and 200 °C), and this would provide larger thermodynamic driven force for formation of NiO. Apparently, this "contradicts" with experiment, which found rather weak NiO signal at RT if there are any. On the other hand, we note that formation of NiO from Pt_3Ni would involve extensive mass transportation and is a highly activated process. The lack of observation of NiO signal at thermodynamically more favorable condition tells that the corresponding process is kinetically hindered at RT. In fact, the presence of the Pt-skin surface before the exposure of oxygen gas can be one possible source of the kinetic hindrance at RT.

Finally, to check the stability of these oxides species under UHV reducing conditions, the O *1s* and Ni *2p* spectra are measured after the gas is being pumped out to UHV at 200 °C, as shown in Fig. 4. As shown from O *1s* spectra of Fig. 4, the intensity of NiO and NiO_x gets decreased significantly while the surface is covered with Ni_2O_3. The Ni *2p* spectra also show identical behaviors as oxygen spectra. It is interesting to note that NiO_x gets reduced completely, suggesting NiO_x and NiO are only being formed under elevated pressure and temperature. However, when the gas is being pumped out to UHV at RT, there is a little change of O *1s* and Ni *2p* spectra found. These results can also be rationalized based on above model. First of all, if the gas is being pumped out to UHV (10^{-9} Torr) at $T = 200\,^{\circ}C$, the corresponding ΔG (−0.19 eV/NiO) becomes less exothermic. This implies that NiO formed becomes less stable and tend to decompose at the elevated temperature, consistent with the significant reduction of the NiO intensity observed. If the oxygen gas is pumped out to UHV (10^{-9} Torr) at RT, the corresponding ΔG (−0.65 eV/NiO) remains considerably exothermic, and NiO formed is thermodynamically rather stable. In addition, the kinetics hindrance at RT becomes severe. Both will prevent the change of O *1s* and Ni *2p* spectra, as indeed found in experiment.

In conclusion, the stability of Pt "skin" surface on Pt_3Ni(1 1 1) alloy is investigated under realistic conditions by using AP-XPS analysis. Even at room temperature, there is a clear indication of Ni segregation to surface under the oxygen pressure of 100 mTorr. As

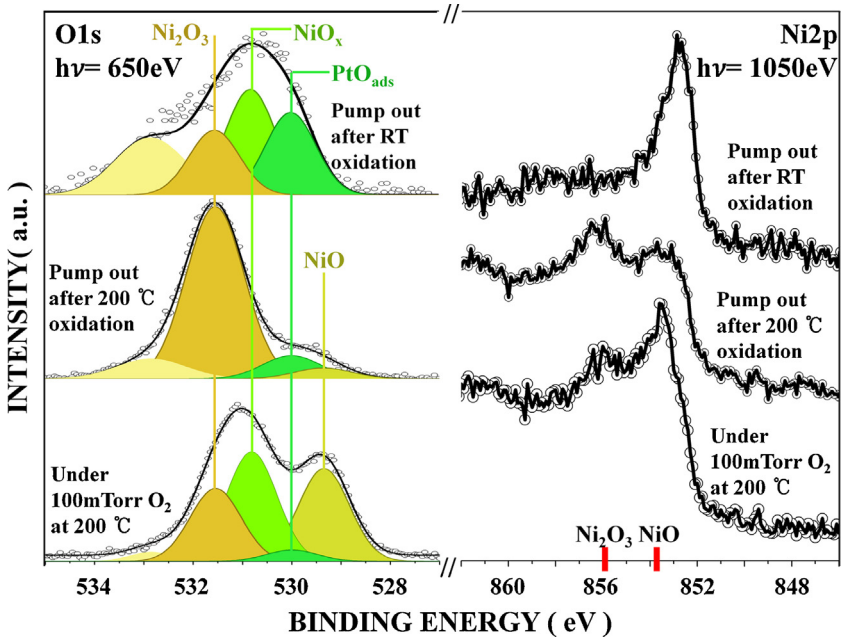

Fig. 4. O *1s* and Ni *2p* core-level spectra measured after oxidation processes. During the evacuation of oxygen gas, the temperature of sample is maintained at $T = 200\,^{\circ}C$ and RT separately.

the temperature increases to 100 °C, the surface segregation and its oxidation of Ni are observed. When the temperature reaches to 200 °C, the formation of disordered NiO and Ni_2O_3 oxides is found on the surface. Interestingly, Pt spectra show a reduction of adsorbed oxygen atoms as the Ni atoms start to appear on the surface, indicating surface segregation between Pt and Ni atoms. The depth profile information indicates that NiO_2 oxide layer is formed at the subsurface region while Ni_2O_3 oxide is being formed at the surface. While the formation of Ni oxides under elevated temperature condition is explained by DFT calculation, yet the kinetic hindrance prevent the formation of NiO at RT.

Acknowledgements

This work was supported by Basic Science Research Program through the National Research Foundation of Korea (NRF) funded by the Ministry of Education, Science and Technology (NRF-2012R1A1A2001745). This work was also supported by GIST College's 2013 GUP Research Fund and MSIP and PAL, XFEL project (SP-12), Korea. WXL was supported by the National Natural Science Foundation of China (21173210 and 21225315) and the National Basic Research Program of China (973 Program, 2013CB834603).

References

[1] V.R. Stamenkovic, B. Fowler, B.S. Mun, G. Wang, P.N. Ross, C.A. Lucas, N.M. Markovic, Science 315 (2007) 493.
[2] V.R. Stamenkovic, B.S. Mun, M. Arenz, K.J.J. Mayrhofer, C.A. Lucas, G. Wang, P.N. Ross, N.M. Markovic, Nat. Mater. 6 (2007) 241–247.
[3] V. Stamenkovic, B.S. Mun, K.J.J. Mayrhofer, P.N. Ross, N.M. Markovic, J. Rossmeisl, J. Greeley, J.K. Norskov, Angew. Chem. Int. Ed. 18 (2006) 2897.
[4] Y.S. Kim, S.H. Jeon, A. Bostwick, E. Rotenberg, P.N. Ross, A.L. Walter, Y.J. Chang, V.R. Stamenkovic, N.M. Markovic, T.W. Noh, S. Han, B.S. Mun, Adv. Energy Mater. 3 (2013) 1267.
[5] K.J.J. Mayrhofer, V. Juhart, K. Hartl, M. Hanzlik, M. Arenz, Angew. Chem. Int. Ed. 48 (2012) 3529.
[6] S.J. Hwang, S.-K. Kim, J.-G. Lee, S.-C. Lee, J.H. Jang, P. Kim, T.-H. Lim, Y.-E. Sung, S.J. Yoo, J. Am. Chem. Soc. 134 (48) (2012) 19508–19511.
[7] H.-Y. Su, X.-K. Gu, X. Ma, Y.-H. Zhao, X.-H. Bao, W.-X. Li, Catal. Today 165 (2011) 89.
[8] D. Sun, Y. Zhao, H. Su, W. Li, Chin. J. Catal. 34 (2013) 1434–1442.
[9] A. Politano, M. Caputo, A. Goldoni, P. Torelli, G. Chiarello, J. Phys. Chem. C 117 (2013) 27007–27011.
[10] C. Chen, Y. Kang, Z. Huo, Z. Zhu, W. Huang, H.L. Xin, J.D. Snyder, D. Li, J.A. Herron, M. Mavrikakis, M. Chi, K.L. More, Y. Li, N.M. Markovic, G.A. Somorjai, P. Yang, V.R. Stamenkovic, Science 343 (6177) (2014) 1339–1343.
[11] A. Toyoshima, H. Tanaka, T. Kikuchi, K. Amemiya, K. Mase, J. Vac. Soc. Jpn. 54 (2011) 580–584.
[12] Z. Hussain, W.R.A. Huff, S.A. Kellar, E.J. Moler, P.A. Heimann, W. McKinney, H.A. Padmore, C.S. Fadley, D.A. Shirley, J. Electron Spectrosc. Relat. Phenom. 80 (1996) 401–404.
[13] M.E. Grass, P.G. Karlsson, B.S. Mun, F. Aksoy, M. Lundqvist, B. Wannberg, Z. Hussain, Z. Liu, Rev. Sci. Instrum. 81 (2010) 053106.
[14] G. Kresse, J. Hafner, Phys. Rev. B 48 (1993) 13115.
[15] G. Kresse, J. Furthmuller, Phys. Rev. B 54 (1996) 11169.
[16] P.E. Blochl, Phys. Rev. B 50 (1994) 17953.
[17] G. Kresse, D. Joubert, Phys. Rev. B 59 (1999) 1758.
[18] J.P. Perdew, J.A. Chevary, S.H. Vosko, K.A. Jackson, M.R. Pederson, D.J. Singh, C. Fiolhais, Phys. Rev. B 46 (1992) 6671.
[19] J. Rossmeisl, A. Logadottir, J.K. Nørskov, Chem. Phys. 319 (2005) 178.
[20] K.S. Kim, N. Winograd, Surf. Sci. 43 (1974) 625.
[21] P.R. Norton, R.L. Tapping, J.W. Goodale, Surf. Sci. 65 (1977) 13.
[22] S. Altieri, L.H. Tjeng, A. Tanaka, G.A. Sawatzky, Phys. Rev. B 61 (2000) 13403.
[23] D.J. Miller, H. Öberg, S. Kaya, H. Sanchez Casalongue, D. Friebel, T. Anniyev, H. Ogasawara, H. Bluhm, L.G.M. Pettersson, A. Nilsson, Phys. Rev. Lett. 107 (2011) 195502.
[24] C.J. Powell, A. Jablonski, NIST Electron Inelastic-Mean-Free-Path Database, Version 1.2, SRD 71, National Institute of Standards and Technology, Gaithersburg, MD, 2010.
[25] R.C. Weast, CRC Handbook of Chemistry and Physics, 5th ed., CRC Press, Cleveland, OH, 1974–1975.
[26] L. Köhler, G. Kresse, M. Schmid, P. Varga, J. Yuhara, X. Torrelles, C. Quiros, J.N. Andersen, Phys. Rev. Lett. 92 (12) (2004) 126102.
[27] W.X. Li, C. Stampfl, M. Scheffler, Phys. Rev. Lett. 90 (2003) 256102.
[28] W.X. Li, C. Stampfl, M. Scheffler, Phys. Rev. B 68 (2003) 165412.
[29] Reuter, M. Scheffler, Phys. Rev. B 65 (2001) 035406.